ESRF	**Experiment title: In Situ Analysis of Nucleant-Mediated Crystallization with Microfluidics-Coupled Micro-Focused X-ray Diffraction**	**Experiment number**: CH 5267
Beamline: ID13	**Date of experiment**: from: 26/11/2017 to: 30/11/2017	**Date of report**: 10/03/2018
Shifts: 9	**Local contact(s)**: Dr. Manfred Burghammer	*Received at ESRF:*

Names and affiliations of applicants (* indicates experimentalists)
M. A. Levenstein*, N. Kapur*, F. C. Meldrum , University of Leeds, United Kingdom

Report:

Beamtime CH5267 made use of our new technique of droplet microfluidics-coupled X-ray diffraction (DMC-XRD). Together, this beamtime and CH4928 allowed us to ***quantify*** the effect of four contrasting insoluble 'nucleant' particles (and seeding with nanoparticles of calcite) on the nucleation of the important model system, calcium carbonate ($CaCO_3$). Experiments at ID13 were performed as described in our previous reports and proposals. Briefly, insert-based microfluidic devices were mounted in the experimental hutch and connected to neMESYS syringe pumps. These pumps supply the fluids and generate a flow of droplets at a T-junction inside the device. The droplets are then directed along a serpentine channel which passes by our analysis window 36 times and allows us to probe these reaction time points with XRD.

Here, we studied the formation of calcite crystals at 50 mM Ca^{2+} and CO_3^{2-} concentrations, in the presence of 0.0017 wt% 58S porous bioglass, NX illite clay, controlled porous glass (CPG), CPG with COOH surface functionalisation, 60 nm calcite particles and without additives. Interestingly, 58S bioglass promoted the growth of calcite almost as quickly as nanocalcite, which is theoretically the most favourable surface for new calcitic growth. Nucleation in the presence of bioglass was first detected at 10.12 ± 2.03 s, as compared to 4.23 s in the presence of nanocalcite (detected from the first analysis position) (Fig. 1a and 1b). However, the overall crystal growth within both populations of droplets reaches a similar quantity (as evidenced by the intensity of diffraction) and slows down at around 40 s for nanocalcite and 60 s for bioglass (Fig. 1c and 1d). NX illite was also shown to promote some calcite growth, but almost no diffraction could be observed from the CPG or control experiments – where these droplets only contained amorphous calcium carbonate (ACC). Subsequent lab-based characterisation (SEM, BET, XRD) of the nucleant particles leads us to conclude that 58S bioglass promotes nucleation due to its level of disorder (wide range of pore sizes and shapes) – meaning that there is higher chance of a pore matching and thus ***stabilising*** the critical nucleus of a crystal.[1] Illite is a naturally occurring material with many pore sizes, so it also nucleates calcite, but to a lesser extent. Synthetic CPGs (with most pores close to 5-6 nm) and even CPGs with COOH functionalisation (which has been shown to promote calcite growth[2]) do not appear to have ***any effect*** on the crystal induction time. These results lend additional support for a 'universal' theory of nucleant-mediated crystallization related to pore-critical nucleus matching and will help us to determine more effective routes to controlling nucleation. A publication on this work and how it relates to similar observations on protein crystallization[1] is currently in preparation.

Additional experiments were also performed to develop the experimental capabilities; SAXS was carried out in combination with WAXS, and new devices with heating capability were investigated. The SAXS and heated experiment data has yet to be processed. However, control experiments to determine the effective detection limit have proved insightful. Figure 2 shows the decay in intensity as a function of concentration of the main Bragg reflection of homogeneous dispersions of magnetite (11 nm) and gold (20 nm) nanoparticles within droplets. Gold, as expected due to its higher electron density and size was detectable below 0.05 wt%, whereas magnetite was only detectable down to 0.3 wt%. Both peaks were lost due to noise in the magnitude of 10^4 arbitrary intensity units, which was based on the 500 frames collected (~187 of which are from the

droplets based on the volume fraction of the dispersed phase). This amounts to noise of roughly 50 arbitrary units per frame. This can be used as a rough estimation of the signal-to-noise ratio based on the background scattering from air, the device windows, solution scattering, and effective noise introduced by the processing routine. With signal lower than this value, we suggest that information could be better obtained through SAXS or total scattering methods. A similar experiment was performed with droplets of 1 wt% 60 nm calcite particles and no Bragg reflections could be observed. This confirms that the signal we detected from the seeded experiment is due to crystal growth and not simply due to detection of the seeds, which at 0.0017% is well below our detection limit.

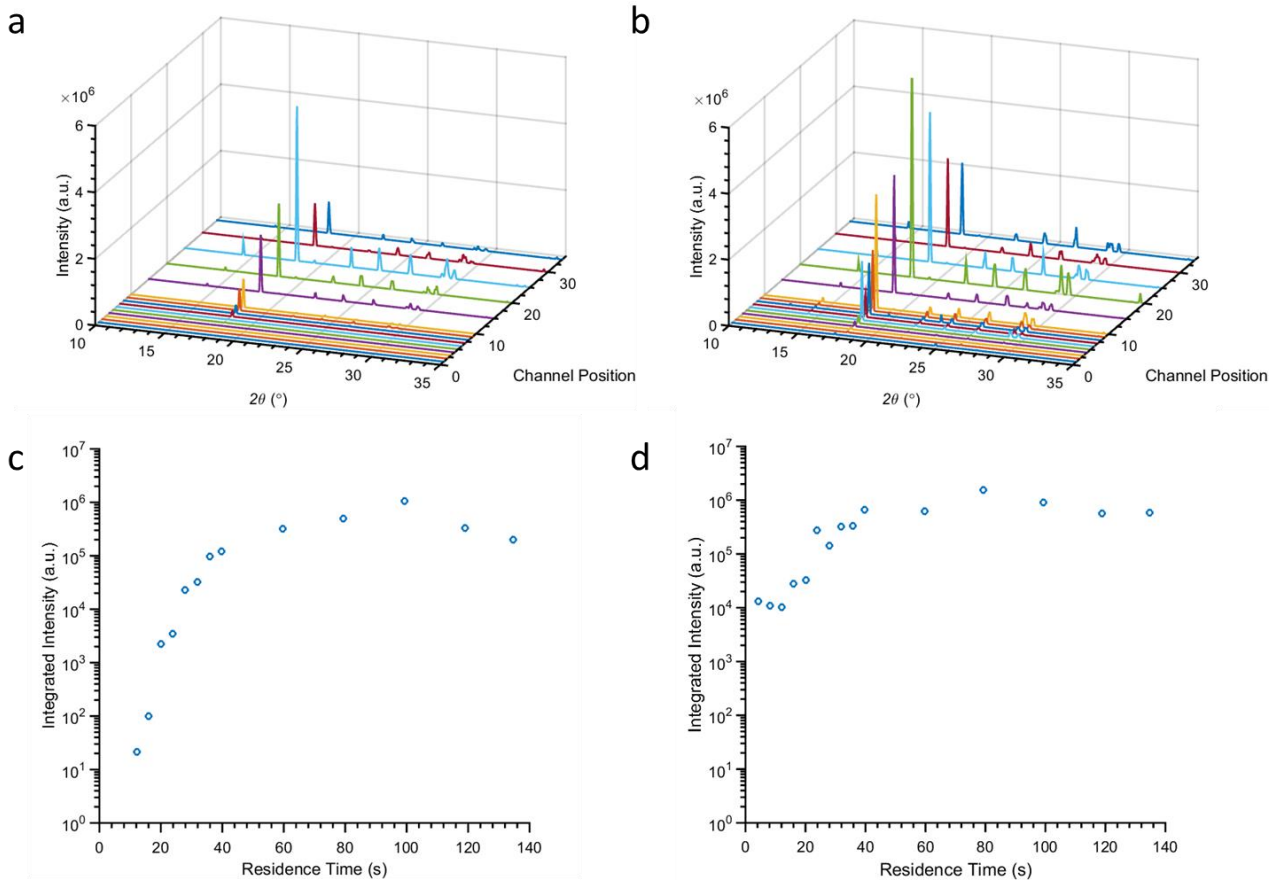

Fig. 1: Diffraction patterns collected from the device as a function of channel position from the (a) 58S bioglass and (b) nanocalcite experiments. (c and d) The integrated intensity of the patterns from a and b, respectively, as a function of solution residence time.

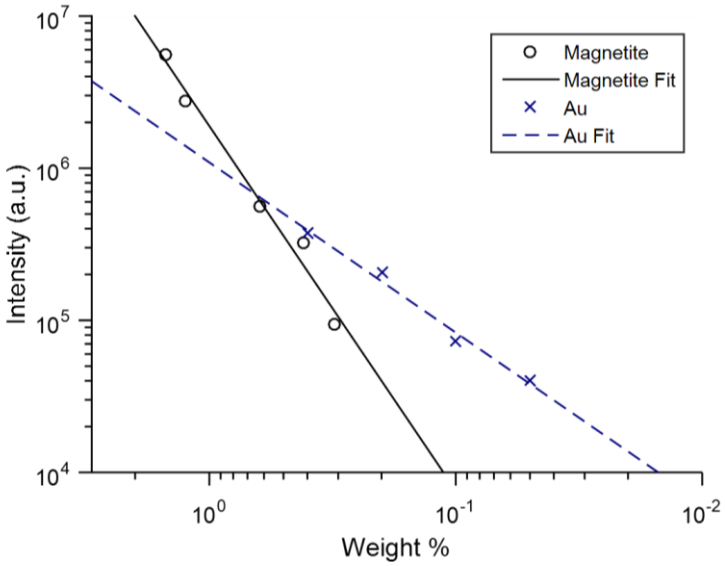

Fig. 2: Diffraction signal decay of nanoparticles measured by the heights of the {311} and {111} reflections of magnetite (Fe_3O_4) and gold (Au), respectively, at their indicated concentration within droplets. The decay appears to follow a logarithmic trend shown by the fit lines.

References: [1] Chayen, Saridakis and Sear, *PNAS*, 2006, **103**, 597. [2] Aizenberg, Black and Whitesides, *Nature*, 1999, **398**, 495.